[5]Carslaw, H. S. and Jaeger, J. C., *Conduction of Heat in Solids*, 2nd ed., Oxford University Press, London, 1959, Chap. 2.
[6]Vallerani, E., "Integral Technique Solution to a Class of Simple Ablation Problems," *Meccanica*, Vol. 9, Jan. 1974, pp. 94-101.
[7]Zien, T. F., "An Integral Approach to Transient Heat-Conduction Problems with Phase Transition," NSWC/WOL/TR 75-37, Naval Surface Weapons Center, White Oak Lab., Silver Spring, Md., March 1975. Also, AIAA Paper 76-171, Wash. D.C., Jan. 1976.

Determination of Stagnation Chamber Temperature in High-Enthalpy Nozzle Flows

Nimai Kuma Mitra*
Deutsche Forschungs-und Versuchsanstalt fuer Luft- und Raumfahrt E.V., Cologne, W. Ger.
and
Martin Fiebig†
Gesamthochschule Duisburg, Duisburg, W. Ger.

Introduction

In high-enthalpy wind-tunnel facilities, the stagnation chamber pressure p_0 and the mass flow rate $\dot{m}$ can be measured directly. The stagnation chamber temperature T_0, which lies typically between 2000 and 5000 K, has to be determined indirectly. This often is done by the simple assumption of inviscid, one-dimensional flow in the subsonic part of the nozzle.[1] For a diatomic gas such as nitrogen, Bachour and Erdtel[2] additionally assumed that the flow was in thermodynamic equilibrium up to the throat and vibrationally frozen thereafter. Carden[3] assumed the flow to be frozen all along the nozzle. The complete neglect of viscous effects in the subsonic part may be questionable in low Reynolds number flow. In particular, the neglect of the wall cooling could lead to substantial error in the T_0 computation. The T_0 calculated from an inviscid flow model in effect replaces an actual nonuniform T_0 profile at the throat by an average uniform one of magnitude smaller than the actual stagnation temperature on the axis at the throat.

Since this computed T_0 generally is used to analyze the flowfield in the uniform core at the nozzle exit from experimental pitot pressure surveys, one may expect significant errors in the calculated test chamber conditions. The purpose of the present note is to suggest an alternative method, based on slender channel analysis,[4] for the calculation of an average stagnation chamber temperature from experimental p_0 and $\dot{m}$. This method takes into account viscous effects, wall cooling, and vibrational relaxation for polyatomic gases in the subsonic part of the nozzle. In connection with thrust calculations for microthruster nozzles, Rae[5] presented a scheme for the numerical solution of slender channel equations with wall-slip boundary conditions for frozen flow. This scheme has been modified and used to calculate flowfields in low Reynolds number hypersonic nozzle where slender channel equations appear to describe the flow adequately.[6,7]

Received Oct. 17, 1975. This work was supported by Deutsche Forschungsgemeinschaft.
Index categories: Boundary Layers and Convective Heat Transfer-Laminar," Nozzle and Channel Flow; Thermal Surface Properties.
*Scientist, Institut fuer Angewandte Gasdynamik. Member AIAA.
†Professor, Fachbereich Maschinenbau und Schiffstechnik.

Governing Equations and Method of Solution

Slender channel equations for two-dimensional and axisymmetric frozen flow have been presented in Refs. 4-7. The equations are formally identical to boundary-layer equations except that the pressure gradient dp/dz along the channel is not known a priori. We present here only a vibrational rate equation, which we obtained by subjecting a modified form of rate equation of Lunkin[8] which takes care of diffusion to slender channel ordering:

$$\rho k \frac{\partial e}{\partial z} + \rho v \frac{\partial e}{\partial r} = \frac{1}{r} \frac{\partial}{\partial r} \left(\frac{\mu r}{Pr_v} \frac{\partial e}{\partial r} \right) + \rho \frac{e_* - e}{\tau} \tag{1}$$

Here e and e_* are vibrational and equilibrium vibrational energies, z and r are axial and normal coordinates, u and v are axial and normal velocities, and ρ and τ are density and local relaxation time, respectively. Pr_v is a vibrational Prandtl number defined as $Pr_v = \mu c_{vib}/k_{vib}$, where μ is a viscosity based on translational temperature, and c_{vib} and k_{vib} are vibrational specific heat and heat conductivity, respectively. Reference 8 has shown that $c_{vib}/k_{vib} = 1/\rho D_{ii}$, where D_{ii} is the coefficient of self-diffusion. For simplicity, we have used $Pr_v = 0.72$.

The wall boundary condition of Eq. (1) is difficult. For "wall-slip," a vibrational temperature condition has been used in Ref. 7. For the no-slip case, we assume a boundary condition, as is the practice for dissociated boundary layers with wall recombination:

$$e - e_{*w} = [(\mu/\alpha_v \rho\, Pr_v)\cos\vartheta(\partial e/\partial r)]_w \tag{2}$$

Here ϑ is the wall inclination angle, subscript w stands for wall, and α_v is the wall catalyticity for vibrational duxcitation and has the dimension of velocity. We notice that $\alpha_v \to \infty$ will mean a perfectly catalytic wall and $e_w = e_{*w}$, and $\alpha_v \to 0$ will mean no vibrational heat exchange with the wall. Following Rae,[5] we derived a stream tube relation from the continuity equation by replacing z derivatives of all flow variables in favor of the axial pressure gradient dp/dz by using momentum, energy, rate, and state (perfect gas) equations. This equation is

$$\partial/\partial r[r(v/u] = B_1(dp/dz) + B_2 \tag{3}$$

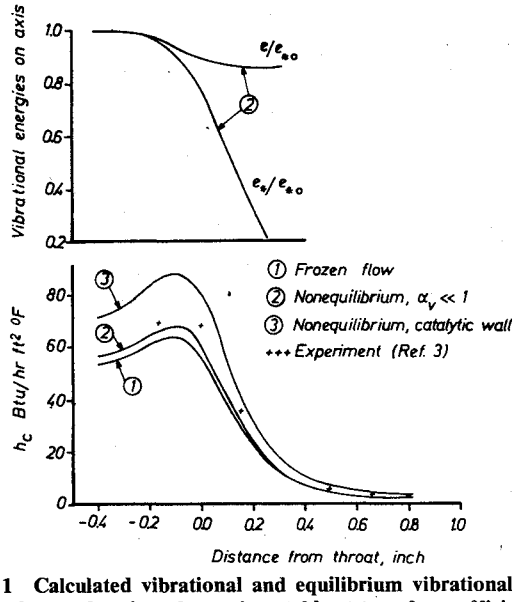

Fig. 1 Calculated vibrational and equilibrium vibrational energies along the nozzle axis and experimental heat-transfer coefficient h_c for nozzle of Ref. 3, run 2.

where

$$B_1 = \left[\frac{1}{\rho u^2} + \frac{1}{\rho h_{tr}} - \frac{1}{p} \right] r$$

$$B_2 = -\frac{1}{\rho u^2} \frac{\partial}{\partial r} \left[\mu r \frac{\partial u}{\partial r} \right] + \frac{1}{\rho u h_{tr}} \frac{\partial}{\partial r} \left[\frac{\mu r}{Pr} \frac{\partial h_{tr}}{\partial r} \right] + \frac{\mu r}{\rho u h_{tr}} \left[\frac{\partial u}{\partial r} \right]^2 - \frac{r}{u h_{tr}} \frac{e_* - e}{\tau}$$

h_{tr} = translational-rotational static enthalpy

Equation (3) was integrated across the nozzle to obtain an expression for the pressure gradient:

$$\frac{dp}{dz} = \frac{r_w (dr_w/dz) + \int_0^{r_w} B_2 dr}{\int_0^{r_w} B_1 dr} = \frac{N(z)}{D(z)} \tag{4}$$

Equation (4) is analogous to the stream-tube relation in one-dimensional inviscid nozzle flow. In a nozzle with given initial boundary conditions, there will be a saddle point where both N and D will become zero when the critical mass flow rate $\dot{m}_c$ is used in the computation. For this mass flow rate, the slender channel equations will have a solution that is supersonic in an average sense when $D<0$. To find this $\dot{m}_c$, Ref. 5 has presented an iteration scheme that finds, for a nozzle with given initial boundary condition, a nondimensional mass flow rate A_{sup} (for supercritical flow) and A_{sub} (for subcritical flow) in such a way that $(A_{sup} - A_{sub}) < 10^{-4}$. Then nondimensional critical mass flow rate is taken as the average of the two. The nondimensional mass flow rate A is defined by the following formula:

$$A = \dot{m} / (2h_0)^{1/2} \rho_0 2\pi r_*^2$$

where r_* is the throat radius, subscript 0 stands for stagnation chamber value, and h is enthalpy. In the present work, the scheme of Rae[5] was used differently, and, instead of finding a new $\dot{m}$ from given p_0 and T_0, we calculated-at each iteration a new T_0 from experimental p_0 and $\dot{m}$. Although in nondimensional flow equations[5,6] the parameters that were functions of p_0 and T_0, such as characteristic Reynolds number Re defined as $(2h_0)^{1/2} r_* \rho_0 / \mu_0$ and for nonequilibrium flow the c_p and characteristic Damkoehler number Q defined as $r_* / (2h_0)^{1/2} \tau_0$), also changed in each iteration, the scheme converged and calculated the desired T_0.

Using finite-difference scheme, the flow equations have been solved numerically. Unlike in Ref. 5, the step-size in normal direction was staggered so that a comparatively large number of steps could be used near the wall for better accuracy and computational economy. The pressure gradient calculation by Eq. (4) breaks down with no-slip boundary condition because of the algebraic singularity in the integrand. This singularity was removed by multiplying Eq. (3) with u^2 and integrating it to obtain an expression for dp/dz. The resulting expression has the same characteristics as Eq. (4). It has been shown elsewhere[9] that this expression of dp/dz for the no-slip case also could be used in the extrapolation scheme through the saddle point, as suggested in Ref. 5. All of the results presented here are for no-slip cases.

To compare with experimental results, we have also calculated the power content P in the flowing gas and the wall heat-transfer coefficient h_c by the following formulas:

$$P = 2\pi \int_0^{r_w} \rho u i r dr$$

where $i = h + (u^2/2)$, and $h_c = (dP/dz) / (T_{aw} - T_w) 2\pi r_w$

where adiabatic wall temperature T_{aw} is obtained from the formula

$$(T_{aw} - T_{ax}) / (T_w - T_{ax}) = (Pr)^{1/2}$$

T_{ax} is the temperature on the axis, T_w is the wall temperature, and Pr is the Prandtl number.

Results and Discussion

We have calculated flowfields in the three nozzles of Refs. 1-3. These nozzles are similar in geometry, with circular subsonic parts and conical supersonic parts. In Ref. 3, Carden presented experimental p_0, $\dot{m}$, and wall heat convection coefficients h_c. Even though the flow medium was nitrogen, Carden[3] calculated T_0 from one-dimensional isentropic frozen flow equations. Table 1 presents our calculated T_0 and estimated values from Refs. 1-3. The isolated influence of heat conduction on T_0 in results of Carden[3] and Papanikas[1] can be seen by comparison with our frozen flow calculations. The differences are 7% and 18%, respectively. We shall make a detailed comparison with experimental results of Carden.[3] The characteristic Damkoehler number Q in this case is 0.275 and 0.285 for noncatalytic and catalytic wall, respectively. For such values of Q, the assumption of frozen flow is questionable. Our calculation with noncatalytic wall shows that vibrational energy constitutes 14% of initial P_0 of 1921.5 J/sec, and of this vibrational energy 16% comes in expansion. The upper half of Fig. 1 shows that the centerline vibrational energy freezes at 86.5% of its stagnation chamber value $5r_*$ downstream of throat. These facts suggest that nonequilibrium calculations should represent the flowfield more accurately. The lower half of Fig. 1 shows that the frozen flow calculation produced values of h_c smaller than the experimental values in the throat region. Interestingly, the experimental h_c values lie between the two nonequilibrium calculations, but closer to the calculated values with noncatalytic wall. We have calculated flow with noncatalytic wall by taking $\alpha_v \ll 1$. Unlike in Ref. 3, no wall temperature was reported in Refs. 1 and 2 in the subsonic part of the nozzle. We have assumed a wall temperature distribution. Figure 2 shows assumed wall temperature, P, and h_c distributions along the nozzle for argon flow.[1] The power loss due to wall

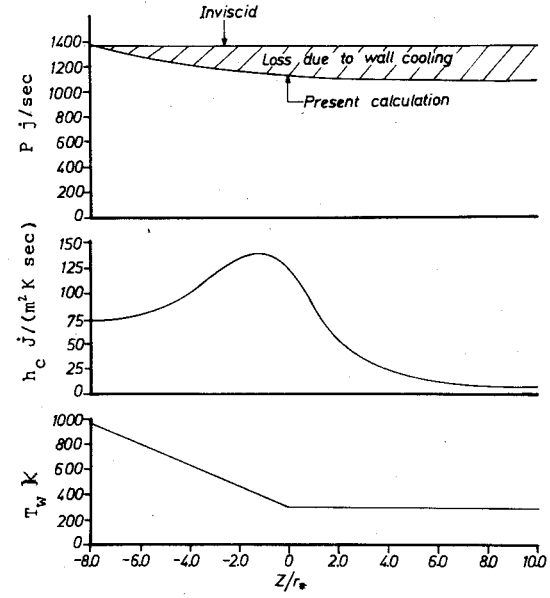

Fig. 2 Wall temperature T_w, wall heat convection h_c, and total power in the gas P along the nozzle with argon flow of Ref. 1.

Table 1 Experimental conditions and calculated T_0 from present work and Refs. 1-3

	Papanikas' nozzle, argon, $p_0 = 0.408$ atm, $\dot{m} = 0.695$ g/sec, T_0,K	Bachour's nozzle, nitrogen, $p_0 = 1$ atm, $\dot{m} = 0.9$ g/sec, T_0K	Carden's nozzle, nitrogen, $p_0 = 1.21$ atm, $\dot{m} = 0.4536$ g/sec, T_0K
One-dimensional isentropic frozen up to throat	3234	...	3373
One-dimensional isentropic equilibrium up to throat	...	2800	2875
Slender channel frozen	3828	...	3598
Slender channel, vibrational nonequilibrium, fully catalytic wall	...	3195	3516
Slender channel, vibrational nonequilibrium, $\alpha_v \ll 1$	...	3179	3486

cooling was 225.5 J/sec, nearly 16.5% of the initial power input. The value of P at the throat was 1135 J/sec, and the average T_0 at the throat was 3140 K, which was quite close to the T_0 calculated from the inviscid flow model.

Flowfields at the nozzle exit computed by the present method have been presented in Refs. 6 and 7. Generally, they compare well with available experimental results. We may conclude by noting that slender channel equations provide a realistic alternative way to calculate average stagnation chamber temperature in high-enthalpy, low Reynolds number frozen or vibrational nonequilibrium nozzle flow from experimentally measurable data of p_0, $\dot{m}$, and nozzle wall temperature. The present method is more time-consuming than simple one-dimensional inviscid approximation but should be recommended for flow with high stagnation temperature where the nozzle wall is subjected to intense cooling. Our calculations show that for such flows the T_0 calculated by the inviscid flow model may lead to error up to 20% for argon and 10% for nitrogen. It also should be noted that zero wall catalyticity for vibrational energy in a cooled-wall nozzle compares better with experiment than fully catalytic wall. Further modifications of the present method to include dissociation of the flow medium are underway.

References

[1] Papanikas, D.G., "Investigations of Axisymmetric Hypersonic Free Jets in High Total Enthalpy Wind Tunnels," ESRO TT-150, March 1975, European Space Research Organization.

[2] Bachour, F. and Erdtel, D., "Experimental Investigations of Hypersonic Low-Density Flows behind Water-cooled and Liquid-Nirtogen-Cooled Nozzles in DFVLR Wing Tunnel PK-1," ESRO TT-129, Feb.1975, European Space Research Organization.

[3] Carden, W. H., "Local Heat-Transfer Coefficients in High-Speed Laminar Flow," *AIAA Journal,* Vol. 3, Dec. 1965, pp. 2183-2189.

[4] Williams, J.C., III, "Viscous Compressible and Incompressible Flow in Slender Channels," *AIAA Journal,* Vol. 1, Jan. 1963, pp. 186-195.

[5] Rae, W. J., "Final Report on a Study of Low-Density Nozzle Flows, with Application to Micro thrust Rockets," CAL AI-2590-A-1, Dec. 1969, Cornell Aeronautical Laboratory, Inc., Buffalo, N.Y.

[6] Mitra, N.K. and Fiebig, M., "Low Reynolds Number Hypersonic Nozzle Flows," *Zeitschrift fur Flugwissenschaften,* Vol. 2, Feb. 1975, pp. 39-45.

[7] Mitra, N.K. and Fiebig, M., "Low Reynolds Number Vibrational Nonequilibrium Flow in Laval Nozzle," *Proceedings of the Ninth International Symposium on Rarefield Gas Dynamics,* July 1974, pp. B.21-1 to B.21-12.

[8] Lunkin, Yu. P., "Vibrational Dissociation Relaxation in a Multicomponent Mixture of Viscous Heat-Conducting Gases," *IUTAM Symposium on Irreversible Aspects of Continuum Mechanics and Transfer of Physical Characteristics in Moving Fluids,* 1966, Vienna, pp. 228-236.

[9] Mitra, N.K. and Fiebig, M., "Flow Field Computation through Sonic Singularity in Viscous Frozen and Ninequlibrium Nozzle Flow," *GAMM Conference on Numerical Methods in Fluid Mechanics,* Oct. 1975, Cologne, West Germany.

Temperature Measurements in Rail Electrode Cross-Flow Arcs

D.M. Benenson* and J.J. Nowobilski†
State University of New York at Buffalo, Buffalo, N.Y.

TEMPERATURE diagnostics in cross-flow arcs have been previously reported for pin electrode configurations operated with an applied transverse magnetic field.[1,2] and in the absence of such a field,[3] i.e., with forced convection alone. The rail electrode arrangement frequently is found in circuit breaker applications; here, interactions of the magnetic field with the arc column play an important role. As an initial step in the study of the time-varying, nonstationary cross-flow arc, the experiments reported herein were carried out upon a steady-state rail electrode configuration, which was maintained stationary (i.e., "balanced" with respect to flow and magnetic effects) through application of a magnetic field transverser to the mainstream flow.

Tests were conducted with a 100 A argon arc operated at about 840 Torr. The mainstream flow velocity ranged from about 3.7 to about 7.3 m/sec; the maximum value of the applied magnetic field was 68 G. Electrode spacing was 1.27 cm. Experiments were conducted in an open-circuit test facility,[1-3] the test section of which was 43 cm long with cross-section

Received Oct. 20, 1975. This research was supported by U.S. Office of Scientific Research Grant 70-1928 and by National Science Foundation Grant ENG74-15272.

Index categories: Plasma Dynamics and MHD; Electric Power Generation Research; Electric and Advanced Space Propulsion.

*Professor, Faculty of Engineering and Applied Sciences.

† Research Assistant, Faculty of Engineering and Applied Sciences; presently Assistant Staff Engineer, Linde Division of Union Carbide, Tonawanda, N.Y.